# Fluorescence spectrum of a two-level atom driven by a multiple modulated field

Z. Ficek,[1,2] J. Seke,[1] A. V. Soldatov,[1,3] and G. Adam[1]
[1]*Institut für Theoretische Physik, Technische Universität Wien, Wiedner Hauptstrasse 8-10/136, A-1040 Wien, Austria*
[2]*Department of Physics and Centre for Laser Science, The University of Queensland, Brisbane, QLD 4072, Australia*
[3]*Department of Statistical Mechanics, V.A. Steklov Mathematical Institute, GSP-1, 117966, Gubkin Street 8, Moscow, Russia*
(Received 19 July 2000; published 11 June 2001)

We investigate the fluorescence spectrum of a two-level atom driven by a multiple amplitude-modulated field. The driving field is modeled as a polychromatic field composed of a strong central (resonant) component and a large number of symmetrically detuned sideband fields displaced from the central component by integer multiples of a constant detuning. Spectra obtained here differ qualitatively from those observed for a single pair of modulating fields [B. Blind, P.R. Fontana, and P. Thomann, J. Phys. B **13**, 2717 (1980)]. In the case of a small number of the modulating fields, a multipeaked spectrum is obtained with the spectral features located at fixed frequencies that are independent of the number of modulating fields and their Rabi frequencies. As the number of the modulating fields increases, the spectrum ultimately evolves to the well-known Mollow triplet with the sidebands shifted from the central component by an effective Rabi frequency whose magnitude depends on the initial relative phases of the components of the driving field. For equal relative phases, the effective Rabi frequency of the driving field can be reduced to zero resulting in the disappearance of fluorescence spectrum, i.e., the atom can stop interacting with the field. When the central component and the modulating fields are 180° out of phase, the spectrum retains its triplet structure with the sidebands located at frequencies equal to the sum of the Rabi frequencies of the component of the driving field. Moreover, we show that the frequency of spontaneous emission can be controlled and switched from one frequency to another when the Rabi frequency or initial phase of the modulating fields are varied.

DOI: 10.1103/PhysRevA.64.013813 PACS number(s): 42.50.Lc, 32.50.+d, 32.80.Qk, 42.50.Gy

## I. INTRODUCTION

The study of spectral properties of the radiation field scattered by an atom is fundamental to a number of research disciplines in optics and laser physics and provides a convenient ground for rigorous examination of the characteristics of atoms and their interaction with the radiation field. It is well known that the fluorescence spectrum of a two-level atom driven by a strong laser field of a constant amplitude consists of three spectral components, known as the Mollow triplet [1], with a central peak located at the frequency of the laser field and two sideband peaks symmetrically shifted from the central peak by the Rabi frequency of the driving field. The sidebands are one and a half times as wide and one third as high as the central peak and the relative widths and heights are independent of the intensity of the laser field. The spectrum reveals the structure of energy levels of the entangled atom-driving field system, and the spectral properties can be understood and conveniently explained in terms of a ''dressed-atom'' description of the atom-field interaction [2]. In the dressed-atom approach, the basic states of the atom plus laser-field system are entangled atom-field states (dressed states). The three components of the fluorescence spectrum are viewed as arising from spontaneous transitions between these entangled states.

Recent theoretical and experimental studies of the interaction of atoms with a time-dependent driving field show that the fluorescence spectrum may be qualitatively different from the standard Mollow triplet that is observed for a constant driving field [3]. The structure of energy levels of the atom plus time-dependent field system depends on the time characteristics of the field and the analysis in this area can be divided into three main groups, including excitations with a sequence of pulses, excitations with continuous phase-modulated or amplitude-modulated fields. In all these cases, the spectra have been found to contain a series of peaks whose positions may not depend on the Rabi frequency of the driving field. In particular, the fluorescence spectrum of a two-level atom driven by an external pulsed field has been studied numerically for different shapes of the pulses [4]. The results show that there are no Rabi sidebands and the detailed structure of the spectrum depends on the duration of the pulse and the number of spectral peaks increases with an increasing area of the pulse. In the case of a phase-modulated excitation, the spectrum exhibits complicated regular, as well as irregular, series of sidebands with the Rabi frequency-dependent peak intensities, separations, and linewidths [5]. In fact, the complexity of the spectra results from the presence of a power broadening and the Stark shift of the spectral resonances.

When the atom is driven by an amplitude-modulated field, the fluorescence spectrum also differs from the Mollow triplet, but is much less complex and displays properties that differ significantly from those found for pulse and phase-modulated excitations [6,7]. Blind *et al.* [6] have analyzed analytically the fluorescence spectrum in an amplitude-modulated field composed of a strong resonant component of frequency $\omega_0$ and two much weaker sidebands (modulators) of frequencies $\omega_0 \pm \delta$. They have found that the spectrum consists of a central component, that is not sensitive to the presence of the modulating fields, and a series of sidebands centered about the Rabi frequency $\Omega_0$ of the resonant field. The sidebands are located at frequencies $\Omega_0 + n\delta$, where $n = \pm 1, \pm 2, \ldots$, and, interestingly, their positions and widths

 

are insensitive to the Rabi frequencies of the driving fields. The number of sidebands, however, increases with an increasing Rabi frequency of the modulating fields. Thus, the spectral lines do not suffer power broadening and the Stark shift, indicating that spontaneous emission from the system occurs at the well-defined frequencies.

Spectra that display some of the same features as those predicted for the pulse excitation or modulated fields have been predicted for a two-level atom driven by a bichromatic field composed of two coherent fields of slightly different frequencies [8]. Furthermore, many other interesting effects have been predicted and observed experimentally, such as subharmonic resonances [9], square-wave oscillations [10], phase-dependent modulations of the Rabi oscillations [11], considerable reduced relaxation (decoherence) rate [12], and gain without population inversion [13].

In this paper, we study the fluorescence spectrum arising from a two-level atom driven by a multiple amplitude-modulated field. The multiple modulated field is formed by combining an odd number of coherent fields of different frequencies with a central (carrier) field of frequency $\omega_0$ and pairs of symmetrically detuned fields (modulators) of frequencies $\omega_0 \pm m\delta$, where $m=1,2,\ldots,(1/2)(N-1)$ and $N$ is the total number of fields. In other words, the multiple modulated field is composed of the carrier component and $(1/2)\times(N-1)$ pairs of modulating sidebands. We use the optical Bloch equations, in which we treat the driving fields classically, and calculate numerically, as well as analytically, the steady-state fluorescence spectrum for different numbers of fields and their Rabi frequencies. We are particularly interested in the sensitivity of the spectrum to a number of pairs of the modulating fields. Following the recent experiments with polychromatic fields [14], one would expect that the fluorescence spectrum should exhibit increasingly more complicated structures with an increasing number of the modulating fields. However, we show that this is not the case and the multipeaked spectrum, found for a single pair of the modulating fields [6,7], reduces to a triplet or may even disappear for a large number of the modulating fields. Moreover, spontaneous emission can be switched from one frequency to another when the Rabi frequencies of the modulating fields and/or their initial phases are varied.

## II. FLUORESCENCE SPECTRUM

### A. General formalism

The incoherent part of the fluorescence spectrum of a radiation field scattered by an atom driven by an external laser field is given by the real part of the Fourier transform of the two-time correlation function of the atomic dipole operators [15]

$$S_{in}(\omega)=\Gamma\,\mathrm{Re}\left(\frac{1}{T}\int_0^T dt\int_0^t dt'\times\langle\Delta\tilde{S}^+(t')\Delta\tilde{S}^-(t)\rangle e^{i(\omega-\omega_0)(t-t')}\right),\qquad(1)$$

where $T$ is the integrating time of the detector,

$$\langle\tilde{S}^{\pm}(t)\rangle=\pm i\langle S^{\pm}\rangle e^{\mp i\omega_L t}\qquad(2)$$

are slowly varying parts of the atomic dipole operators,

$$\Delta\tilde{S}^{\pm}(t)=\tilde{S}^{\pm}(t)-\langle\tilde{S}^{\pm}(t)\rangle\qquad(3)$$

are the fluctuation operators, and $\omega_L$ is the laser frequency, which we assume to be exactly tuned to the atomic transition frequency $\omega_0$.

The atom is modeled as a two-level system with the ground-state $|1\rangle$ and the excited-state $|2\rangle$ separated by the transition-frequency $\omega_0$. We assume that the atom is driven by a coherent multimode field and also is coupled to the remaining modes of the three-dimensional electromagnetic (EM) field, which are in the vacuum state. The coupling to the vacuum field leads to spontaneous emission with a rate $\Gamma$. The multimode driving field is taken as a multifrequency modulator with the amplitude

$$\vec{E}(t)=\frac{1}{2}\sum_{n=-p}^{p}\vec{E}_n(t)e^{-i(\omega_n t+\psi_n)}+\text{c.c.}$$

$$=\frac{1}{2}e^{-i(\omega_0 t+\psi_0)}\sum_{n=-p}^{p}\vec{E}_n(t)e^{-i(\delta_n t+\phi_n)}+\text{c.c.},\qquad(4)$$

where $\vec{E}_n(t)$ and $\omega_n$ are the amplitude and frequency of the $n$th component, respectively, $\delta_n=\omega_n-\omega_0$ is the beat frequency (detuning) between $n\neq 0$ and the carrier $(n=0)$ field, $2p+1=N$ is the number of the field components, $\psi_n$ is the initial phase of the $n$th component, and $\phi_n=\psi_n-\psi_0$ is the relative initial $(t=0)$ phase between the carrier and the sideband fields. Further on we assume that $\psi_0=0$.

The two-time correlation functions of the atomic dipole operators can be found from the optical Bloch equations, which can be written in a matrix form as

$$\frac{d}{dt}Y(t,t')=\mathcal{M}(t)Y(t,t'),\qquad(5)$$

where $Y(t,t')$ is a column vector with the components

$$Y_1(t,t')=\langle\tilde{S}^+(t')\tilde{S}^-(t)\rangle-\langle\tilde{S}^+(t')\rangle\langle\tilde{S}^-(t)\rangle,$$

$$Y_2(t,t')=\langle\tilde{S}^+(t')\tilde{S}^+(t)\rangle-\langle\tilde{S}^+(t')\rangle\langle\tilde{S}^+(t)\rangle,$$

$$Y_3(t,t')=\langle\tilde{S}^+(t')\tilde{S}^z(t)\rangle-\langle\tilde{S}^+(t')\rangle\langle\tilde{S}^z(t)\rangle,\qquad(6)$$

$\mathcal{M}(t)$ is the $3\times 3$ matrix

$$\mathcal{M}(t)=\begin{pmatrix}-\frac{1}{2}\Gamma & 0 & \Omega(t)\\ 0 & -\frac{1}{2}\Gamma & \Omega^*(t)\\ -\frac{1}{2}\Omega^*(t) & -\frac{1}{2}\Omega(t) & -\Gamma\end{pmatrix},\qquad(7)$$

and

$$\Omega(t)=\vec{\mu}\cdot\vec{E}(t)/\hbar \tag{8}$$

is the Rabi frequency of the multiple-modulated field and $\vec{\mu}$ is the dipole matrix element of the atomic transition.

In general, the time dependence of the Rabi frequency $\Omega(t)$ is quite complicated and, according to Eq. (4), involves $N$ different parameters $\delta_n$. The analytic description of such a problem is extremely difficult. The problem simplifies when the frequencies of the field components are equidistant and symmetrically distributed about the central frequency $\omega_0$, such that $\delta_n=n\delta$. In this special case, the mode frequencies are integer multiplies of a single parameter $\delta$

$$\Omega(t)=\Omega_0+2\sum_{n=1}^{p}\Omega_n e^{-i\phi_n}\cos n\delta t, \tag{9}$$

where we have assumed that $\phi_{-n}=\phi_n$ and $\Omega_{-n}=\Omega_n$.

It is seen from Eq. (9) that the symmetrically detuned sideband fields act as a modulator of the Rabi frequency $\Omega_0$ of the central component. Depending on the phase $\phi_n$, the sideband fields can modulate the amplitude or the phase of $\Omega_0$. For $\phi_n=0$ or $\pi$, the sidebands modulate the amplitude of $\Omega_0$

$$\Omega(t)=\Omega_0\left(1\pm\sum_{n=1}^{p}a_n\cos n\delta t\right), \tag{10}$$

where $a_n=2\Omega_n/\Omega_0$ is the modulation amplitude and the sign ''+'' corresponds to $\phi_n=0$, while ''−'' corresponds to $\phi_n=\pi$.

For $\phi_n=\pi/2$ or $3\pi/2$, the sideband fields modulate the phase of $\Omega_0$ as

$$\Omega(t)=\Omega_0\left(1\mp i\sum_{n=1}^{p}a_n\cos n\delta t\right). \tag{11}$$

In the following, we focus on the amplitude-modulated field of the form (10), and present numerical, as well as analytical, solutions for the incoherent fluorescence spectrum. In the course of previous work on fluorescence spectra in amplitude-modulated fields, only the case of a single pair $(n=1)$ of the modulating fields has been studied [6,7]. Here, we extend the calculations to the case of a multiple modulation $(n>1)$ and, in particular, we focus on the opposite limit of a large number of modulating fields.

### B. Calculation of the spectrum

To illustrate the effect of a multiple modulation on the incoherent fluorescence spectrum $S_{in}(\omega)$, we numerically solve Eq. (5). We give some of the details of the numerical method in Appendix A and the analytical calculations in Appendix B.

According to Eqs. (1) and (A1), the incoherent fluorescence spectrum can be calculated as the real part of the zeroth-order harmonic of the $Y_1(z)$ component

$$S_{in}(\omega)=\Gamma\,\mathrm{Re}\,Y_1^{(0)}(z)\big|_{z=-i(\omega-\omega_0)}, \tag{12}$$

where

$$Y_1^{(0)}(z)=\frac{1}{P_0(z)}\left(Y_1^{(0)}(0)+\sum_{n=-p}^{p}\tilde{\Omega}_n Y_3^{(-n)}(z)\right). \tag{13}$$

The expression (13) involves the quantities $Y_3^{(-n)}(z)$ which are found from the recurrence relation (A3) by using the truncated basis of the harmonic amplitudes. The validity of the truncation is ensured by requiring that $Y_3^{(-n)}$ does not change as the number of truncated harmonics is increased or decreased by one. Thus, the fluorescence spectrum can be evaluated using the result (13) to any desired accuracy and for an arbitrary number of modulating fields.

Before discussing the influence of a multiple modulation on the fluorescence spectrum, let us briefly recall the basic features of the spectrum in a monochromatic $(p=0)$ field and in an amplitude-modulated field with a single pair $(p=1)$ of the modulating fields. The fluorescence spectrum for a strong monochromatic driving field was predicted by Mollow [1] and consists of a central peak located at the frequency $\omega_0$ of the driving field and two sidebands, symmetric about $\omega_0$, and located at $\omega_0\pm\Omega_0$, where $\Omega_0$ is the Rabi frequency of the driving field. The spectrum has been experimentally observed by various groups [16]. The fluorescence spectrum for an amplitude-modulated field with a single pair of the modulating fields has been calculated by Blind *et al.* [6] (see also Ref. [7]). They have shown that in the modulated field, the spectrum consists of a single central component at $\omega_0$ and a series of sidebands centered about $\pm\Omega_0$ and located at frequencies $\Omega_0+n\delta$, where $n=0,\pm1,\pm2,\ldots$, and $\delta$ is the modulation frequency. The positions of the sidebands are independent of the amplitude $\Omega$ of the modulating fields, but the number of sidebands increases with increasing $\Omega$. The multipeak structure of the spectrum has been interpreted in terms of parametric resonances that the modulation introduces nonlinear oscillations into the average atomic populations and dipole moments at frequencies $\Omega_0+n\delta$.

We now present the numerical results for the fluorescence spectrum of a two-level atom driven by a multiple modulated field. In Fig. 1, we plot $S_{in}(\omega)$ for a weak modulation with $\Omega_0=40\Gamma$, $\Omega_n=\Omega=\pm5\Gamma$, $\delta=5\Gamma$ and two different numbers of pairs $p$ of the modulating fields: $p=1$ [Fig. 1(a)] and $p=2$ [Fig. 1(b)]. Since the spectrum is symmetrical about $\omega_0$, we present only one side of the spectrum for positive $\omega-\omega_0$. For both values of $p$, the spectrum displays a multiplet structure centered about $\Omega_0$. The peaks are located at $\Omega_0+n\delta$ and their positions are independent of $p$. For a single pair of the modulating fields $(p=1)$, the structure is symmetrical about $\Omega_0$ and not sensitive to the sign of the modulation amplitude. However, for the case of two pairs of the modulating fields $(p=2)$, the structure is strongly asymmetric about $\Omega_0$ and displays a strong peak at $\Omega_0-\delta$. Furthermore, the peaks ''flip'' about $\Omega_0$ when $\Omega\rightarrow-\Omega$.

We can explain the ''flip'' effect by analyzing the dependence of the amplitude of the spectral line at $\Omega_0+\delta$ on the sign of $\Omega$. From the analytical solution (B12), we find that only the terms with $q_1+2q_2=1$ and $r_1+2r_2+1=0$ contrib-

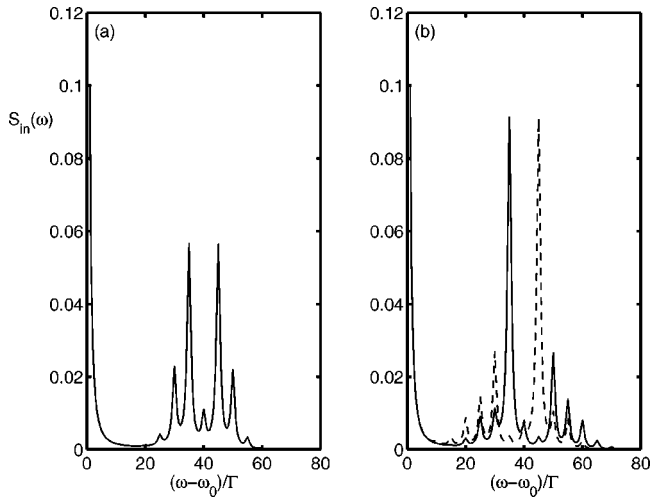


FIG. 1. Fluorescence spectrum for $\Omega_0=40\Gamma$, $\delta=5\Gamma$, $\Omega=5\Gamma$ (solid line), $\Omega=-5\Gamma$ (dashed line), and (a) $p=1$, (b) $p=2$.

ute to the amplitude of the line. In this case, the amplitude of the line $I(\Omega_0+\delta)$ is governed by the following combination of the Bessel functions

$$I(\Omega_0+\delta)=J_{-(2q_2-1)}(A_1)J_{-(2r_2+1)}(-A_1)J_{q_2}(A_2)\times J_{r_2}(-A_2). \quad (14)$$

The expression (14) can be divided into four terms depending on whether $q_2$ and $r_2$ are even or odd numbers, namely, we can divide Eq. (14) into a sum of even-even, odd-odd, even-odd, and odd-even terms. It is easily verified that the even-even and odd-odd terms are invariant under the change $\Omega\rightarrow-\Omega$. However, the even-odd and odd-even terms change the sign to opposite when $\Omega\rightarrow-\Omega$. Thus, depending on the sign of $\Omega$, the even-odd and odd-even terms can enhance or reduce the amplitude of the spectral line.

A similar calculation of the amplitude of the spectral line at $\Omega_0-\delta$ predicts that the amplitude can be obtained from Eq. (14) by changing $A_1\rightarrow-A_1$ and $A_2\rightarrow-A_2$. Thus, the even-odd and odd-even terms contribute to the amplitude of the line at $\Omega_0-\delta$ with opposite sign to that of the line at $\Omega_0+\delta$. These simple considerations of the amplitudes of the spectral lines, based on the properties of the Bessel functions, clearly explain the dependence of the spectrum on the sign of $\Omega$ and the flip of the spectral lines about $\Omega_0$ when $\Omega\rightarrow-\Omega$.

Figure 2 illustrates the transition from the monochromatic driving field case treated by Mollow [1] to a more general case of multiple-modulated fields. The Rabi frequencies of the carrier and the modulating fields are fixed at $\Omega_0=40\Gamma$ and $\Omega=10\Gamma$, respectively, while the number of pairs $p$ of the modulating fields is varied from 0 to 50. With $p=0$, the incoherent spectrum is the Mollow triplet with the sideband peaks located at $\pm\Omega_0$. As the number of the modulating fields increases, the Rabi sidebands split into multiplets. Surprisingly, when we further increase the number of the modulating fields, the multiple sidebands ''return'' to single peaks, similar to the Mollow sidebands, but with the frequencies shifted towards the central peak by $\Omega$. Thus, for a large number of the modulating fields, the total driving field acts as a pair of coherent fields with Rabi frequencies $\Omega_0$ and $\Omega$ and 180° out of phase. This results in the disappearance of the resonance fluorescence when $\Omega=\Omega_0$.

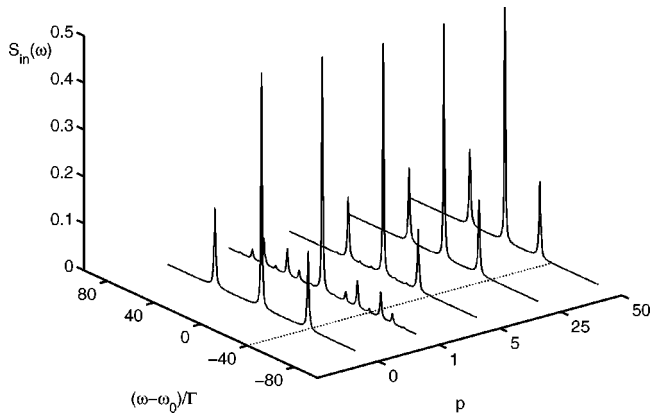


FIG. 2. Fluorescence spectrum versus $\omega-\omega_0$ and $p$, for $\Omega_0=40\Gamma$, $\delta=10\Gamma$, and $\Omega=10\Gamma$.

The shift of the sidebands depends on the amplitude $\Omega$ of the modulating fields. This is shown in Fig. 3, where we plot the spectrum for $\Omega_0=40\Gamma, \delta=5\Gamma, p=25$, and different $\Omega$. The most striking feature of the spectrum is that the single sidebands appear whenever $\Omega=m\delta$, where $m=1,2,\ldots$, and multipeak sidebands are observed when $\Omega\neq m\delta$. Thus, for a large number of the modulating fields, the system retains its periodic structure with resonances at fixed frequencies $\Omega_0\pm n\delta$, but can radiate only at one of the sideband frequencies. In other words, spontaneous emission into the sideband resonances can be controlled by the Rabi frequency $\Omega$ of the modulating field. This is in contrast to the case of $p=1$, where the number of excited resonances increases with increasing $\Omega$. When $\Omega=m\delta$, the triplet spectrum has the same properties as the Mollow triplet, with the intensity ratio 3:1 of the central peak to the sidebands, and the linewidths $1/2\Gamma$ and $3/4\Gamma$, respectively.

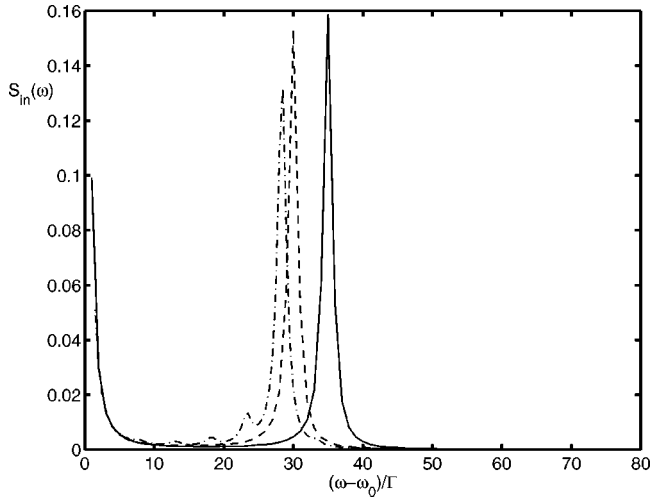


FIG. 3. Fluorescence spectrum for $\Omega_0=40\Gamma, \delta=5\Gamma$, $p=25$, and different $\Omega$: $\Omega=5\Gamma$ (solid line), $\Omega=10\Gamma$ (dashed line), $\Omega=12.5\Gamma$ (dashed-dotted line).

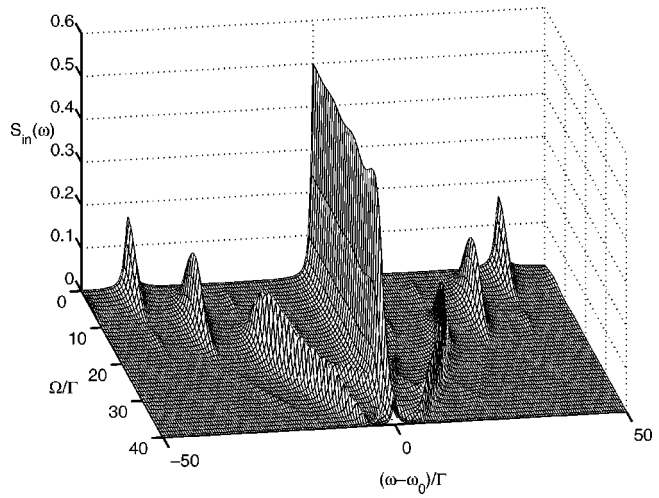


FIG. 4. Three-dimensional spectra versus $\omega-\omega_0$ and positive $\Omega$, for $\Omega_0=40\Gamma$, $\delta=10\Gamma$, and $p=25$.

We plot three dimensional spectra for $\Omega_0=40\Gamma, \delta=10\Gamma$, and $p=25$ in Figs. 4 ($\Omega>0$) and 5 ($\Omega<0$) to further demonstrate the control and the transfer of spontaneous emission between the harmonic resonances. Figure 4 shows that with the increasing $\Omega$, the frequency of spontaneous transitions shifts towards the central peak and the fluorescence disappears when $\Omega=\Omega_0$. Figure 5 shows that with negative values of $\Omega$, the frequency of the spontaneous transitions shifts towards the resonances away from the central peak.

The transfer of spontaneous transitions from one resonance to only the neighboring resonance suggests that interesting modifications of the spectrum can be observed when $\delta=\Omega_0$. In this case, the nearest resonance to the Rabi sideband coincides with the central component of the spectrum and the sidebands at $\pm 2\Omega_0$. Therefore, with increasing (negative) $\Omega$, the spontaneous transitions occurring at the Rabi sidebands could be completely transferred to the sidebands at $\pm 2\Omega_0$. We show this in Fig. 6, where we plot three-dimensional spectra for $\delta=\Omega_0=40\Gamma, p=25$, and negative $\Omega$. In this case, the modulating fields act as a monochromatic field oscillating in phase with the central component. Thus, spontaneous emission from a two-level atom can be controlled by the modulated field and can be switched from one frequency to another, e.g., from the Rabi resonances to the resonances at twice Rabi frequency.

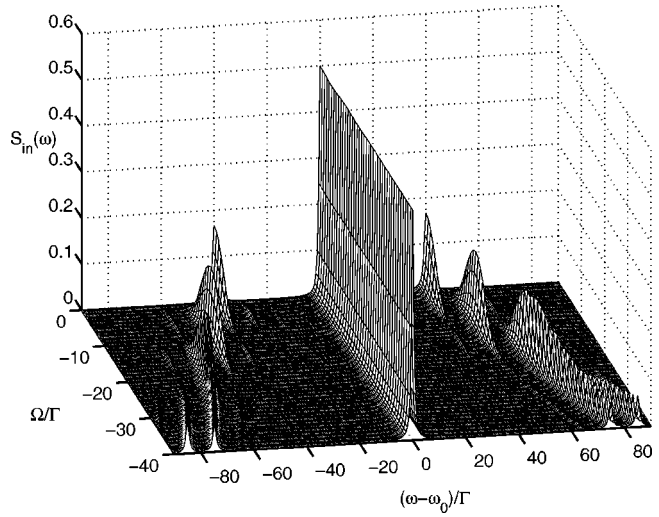


FIG. 5. Same as in Fig. 4, but with negative $\Omega$.

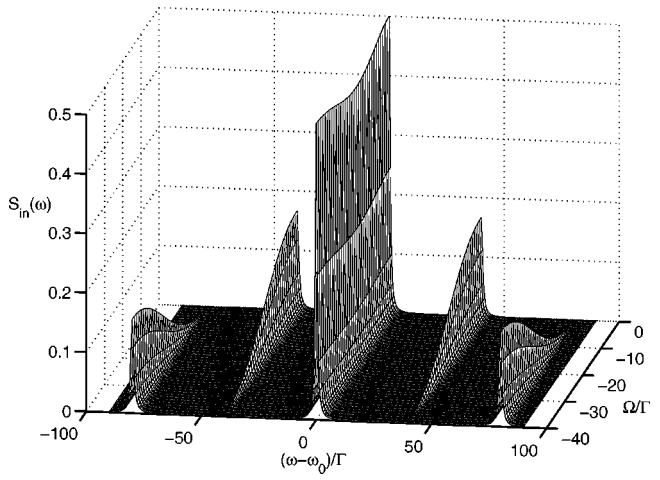


FIG. 6. Three-dimensional spectra for $\Omega_0=\delta=40\Gamma$, $p=25$, and with negative $\Omega$.

The properties of the spectrum for a large number of modulating fields, presented in Figs. 2–6, are difficult to explain from the analytical solution (B9). Therefore, we take a different theoretical approach. In the case of a very large number of fields ($N\gg 1$), we can approximate the sums over $n$, appearing in Eq. (B4), by [17]

$$\sum_n A_n(\sin n\delta t' - \sin n\delta t) \approx \Omega(t-t'). \tag{15}$$

When we substitute Eq. (15) into Eq. (B4), we then obtain the spectrum in the form

$$S_{in}(\omega)=\frac{1}{8}\Gamma^2\left[1-\frac{3}{4}\frac{\Gamma^2}{(\frac{3}{4}\Gamma)^2+(\Omega_0-\Omega)^2}\right]\times\left\{\frac{1}{\frac{1}{4}\Gamma^2+(\omega-\omega_0)^2}+\frac{3}{4}\frac{1}{\frac{9}{16}\Gamma^2+(\omega-\omega_0+\Omega_0-\Omega)^2}+\frac{3}{4}\frac{1}{\frac{9}{16}\Gamma^2+(\omega-\omega_0-\Omega_0+\Omega)^2}\right\}. \tag{16}$$

One can see that the spectrum is a triplet, similar to the well-known Mollow triplet predicted for a monochromatic driving field. However, the sidebands are located at the ''effective'' Rabi frequency of the multiple-modulated field that is equal to the difference $\Omega_0-\Omega$. Thus, a strong modulated field with a large number of frequency components acts as two monochromatic fields of the Rabi frequencies $\Omega_0$ and $\Omega$ and shifted 180° in phase. When $\Omega=\Omega_0$, these two fields

destructively interfere resulting in the disappearance of the resonance fluorescence. Thus, the atom remains in its ground state despite that it is continuously driven by a strong field [18]. When we change $\Omega \rightarrow -\Omega$, the effective Rabi frequency changes to $\Omega_0 + \Omega$. In this case, the spectrum remains a triplet with the sidebands located at $\pm(\Omega_0 + \Omega)$. It is seen that the numerical results presented in Figs. 4–6, are in good agreement with the analytical expression (16).

## III. SUMMARY

We have presented a detailed analysis of the fluorescence spectrum for a two-level atom driven by an amplitude-modulated field composed of a large number of frequency components. We have shown that the fluorescence spectrum arising from an atom driven by a multiple-modulated field is very different from that arising from an atom driven by a single pair of the modulating fields as discussed by Blind *et al*. [6]. With a weak modulation amplitude, the multipeak spectrum displayed when the atom is driven by a single pair of the modulating fields becomes a triplet with a multiple-modulated field. In addition, with an increasing of the modulation amplitude, the atom collapses to the ground state and the fluorescence turns off. We have also shown that the sidebands can switch from one to another by changing the initial phase and the amplitude of the modulating fields. The current study provides a clear physical picture of a multiple-modulated field interacting with an atom, and can be applied to control spontaneous emission in atomic systems and may also prove very useful in the more complicated problem of coherent control of a quantum system. The goal in coherent control is to guide the evolution of a system along a particular path to a desired final state. In our system, the evolution can be controlled by the amplitude and frequency of the modulating fields, and the system can radiate only at desired frequencies.

Finally, we conclude with a brief comment on the possibility of experimental observation of these novel features. The essential conditions for these effects is that the atom is driven by a large number of fields of different but equidistant frequencies. Of course, it would be difficult to focus a large number of separate laser fields on a single atom, although experiments with four driving fields have already been reported [14]. Alternatively, this system could be realized by applying a multimode symmetric mode-locked laser [19], or by applying electro-optic modulation of a single-mode laser. The output from the modulator is a polychromatic field composed of many equidistant frequency components. Therefore, the experimental observation of these effects is feasible.

## ACKNOWLEDGMENTS

This work has been supported by the Jubiläumsfonds der Oesterreichischen Nationalbank zur Förderung der Forschungs- und Lehraufgaben der Wissenschaft under Contract No. 7720. A.V.S. acknowledges support from the RFBR program of Support for Leading Scientific Schools, Grant No. 00-15-96149 and would also like to thank the Österreichische Akademie der Wissenschaften for the invitation and financial support to visit the Institut für Theoretische Physik, Technische Universität Wien.

## APPENDIX A: NUMERICAL SOLUTION

In this appendix, we outline the numerical method for calculating the incoherent part of the fluorescence spectrum of a two-level atom driven by a multiple-modulated field.

In the numerical approach, we use the Floquet method [20], in which the atomic dynamics are described in terms of Fourier components of the dipole correlation functions. In this approach, we make a harmonic decomposition of the expectation values [20]

$$Y_k(t,t') = \sum_{l=-\infty}^{\infty} Y_k^{(l)}(t,t') e^{il\delta t}, \quad k=1,2,3, \tag{A1}$$

where $Y_k^{(l)}(t,t')$ are slowly varying harmonic components of $Y_k(t,t')$. The harmonic decomposition (A1) tells us that the atomic variables will respond at harmonics of the modulation frequency, and knowledge of $Y_k^{(l)}$ gives all the information about the evolution of the two-time correlation functions.

Substituting Eq. (A1) into Eq. (5) and comparing coefficients of the same powers in $l\delta$, we obtain the following equations of motion for the harmonic components

$$\frac{d}{dt}Y_1^{(l)} = -\left(\frac{1}{2}\Gamma + il\delta\right)Y_1^{(l)} + \sum_{n=-p}^{p} \tilde{\Omega}_n Y_3^{(l-n)},$$

$$\frac{d}{dt}Y_2^{(l)} = -\left(\frac{1}{2}\Gamma + il\delta\right)Y_2^{(l)} + \sum_{n=-p}^{p} \tilde{\Omega}_n^* Y_3^{(l+n)},$$

$$\frac{d}{dt}Y_3^{(l)} = -(\Gamma + il\delta)Y_3^{(l)} - \frac{1}{2}\sum_{n=-p}^{p} \tilde{\Omega}_n^* Y_1^{(l+n)} - \frac{1}{2}\sum_{n=-p}^{p} \tilde{\Omega}_n Y_2^{(l-n)}, \tag{A2}$$

where $\tilde{\Omega}_n = \Omega_n e^{-i\phi_n}$.

Taking the Laplace transform of Eq. (A2) and eliminating $Y_1^{(l)}(z)$ and $Y_2^{(l)}(z)$, the set of equations (A2) can be written in a form of an inhomogeneous $(2N-1)$-term recurrence relation for $Y_3^{(l)}(z)$ as

$$(z+\Gamma+il\delta)Y_3^{(l)}(z) + \frac{1}{2}\sum_n \sum_m \frac{\tilde{\Omega}_n^* \tilde{\Omega}_m}{P_{l+n}(z)} Y_3^{(l+n-m)}(z) + \frac{1}{2}\sum_n \sum_m \frac{\tilde{\Omega}_n \tilde{\Omega}_m^*}{P_{l-n}(z)} Y_3^{(l-n+m)}(z) = g_l(z), \tag{A3}$$

where $P_l(z) = z + (1/2)\Gamma + il\delta$, $z$ is a complex (Laplace transform) parameter, and

$$g_l(z)=Y_3^{(l)}(0)-\frac{1}{2}\sum_n \frac{\tilde{\Omega}_n^*}{P_{l+n}(z)}Y_1^{(l+n)}(0)$$

$$-\frac{1}{2}\sum_n \frac{\tilde{\Omega}_n}{P_{l-n}(z)}Y_2^{(l-n)}(0) \tag{A4}$$

is an inhomogeneous term given by the initial values of the atomic correlation functions

$$Y_1^{(l)}(0)\equiv Y_1^{(l)}(t',t')=\frac{1}{2}\delta_{l,0}+X_3^{(l)}(t')$$

$$-\sum_{r=-\infty}^{\infty} X_1^{(l-r)}(t')X_2^{(r)}(t'),$$

$$Y_2^{(l)}(0)\equiv Y_2^{(l)}(t',t')=-\sum_{r=-\infty}^{\infty} X_2^{(l-r)}(t')X_2^{(r)}(t'),$$

$$Y_3^{(l)}(0)\equiv Y_3^{(l)}(t',t')=-\sum_{r=-\infty}^{\infty}\left(\frac{1}{2}\delta_{r,0}+X_3^{(r)}(t')\right)X_2^{(l-r)}(t'). \tag{A5}$$

In Eq. (A5), $X_k^{(l)}$ are stationary harmonic amplitudes of the components of the Bloch vector given in terms of the expectation values of the atomic variables

$$X_1(t')=\langle\tilde{S}^-(t')\rangle=\sum_{l=-\infty}^{\infty} X_1^{(l)}(t')e^{il\delta t'},$$

$$X_2(t')=\langle\tilde{S}^+(t')\rangle=\sum_{l=-\infty}^{\infty} X_2^{(l)}(t')e^{il\delta t'},$$

$$X_3(t')=\langle\tilde{S}^z(t')\rangle=\sum_{l=-\infty}^{\infty} X_3^{(l)}(t')e^{il\delta t'}, \tag{A6}$$

and $\delta_{l,0}$ is the Kronecker delta function. It is not difficult to show that the stationary (time-independent) solutions for the Fourier harmonics $X_k^{(l)}$ can be found from the system of equations of motion being similar to Eq. (6). In particular, the $X_3^{(l)}$ components satisfy the same recurrence relation as Eq. (A3), but with $z=0$ and $g_l(z)$ replaced by $-(1/2)\Gamma\delta_{l,0}$.

The recurrence relation (A3) is valid for an arbitrary number of fields and for arbitrary values of Rabi frequencies and detunings $\delta$. For $p=1$, the relation (A3) reduces to the well-known recurrence relation for a trichromatic field, which, for $\phi_1=\phi_{-1}=0$ or $\pi$, is equivalent to an amplitude-modulated field with a single pair of the modulating fields [6,7].

## APPENDIX B: ANALYTICAL SOLUTION

In this appendix, we derive analytical expression for the fluorescence spectrum in the limit of a strong driving field. We use the method initiated by Blind *et al.* [6] for a single-modulated Rabi frequency, and extend their approach to the case of a multiple-modulated Rabi frequency. In this approach, we introduce the following linear combinations of the two-time expectation values of the atomic operators

$$V(t,t')=\frac{1}{2}[Y_1(t,t')-Y_2(t,t')],$$

$$U(t,t')=Y_3(t,t')+\frac{i}{2}[Y_1(t,t')+Y_2(t,t')],$$

$$W(t,t')=Y_3(t,t')-\frac{i}{2}[Y_1(t,t')+Y_2(t,t')], \tag{B1}$$

where $Y_k(t,t')$ are defined in Eq. (6). Using the optical Bloch equations (5), we find that the equations of motion for the linear combinations $V(t,t'),U(t,t')$ and $W(t,t')$ are

$$\frac{d}{dt}V(t,t')=-\frac{1}{2}\Gamma V(t,t'),$$

$$\frac{d}{dt}U(t,t')=-\frac{3}{4}\Gamma U(t,t')-\frac{1}{4}\Gamma W(t,t')+i\Omega(t)U(t,t'),$$

$$\frac{d}{dt}W(t,t')=-\frac{3}{4}\Gamma W(t,t')-\frac{1}{4}\Gamma U(t,t')-i\Omega(t)W(t,t'), \tag{B2}$$

where $\Omega(t)$ is given in Eq. (10).

It follows from Eq. (B2) that $V(t,t')$ is independent of the driving field and is decoupled from the remaining components. Its solution has the simple exponential form

$$V(t,t')=V(t',t')e^{-(1/2)\Gamma(t-t')}, \tag{B3}$$

where $V(t',t')$ is the initial value of $V(t,t')$.

The remaining components $U(t,t')$ and $W(t,t')$, which depend on the driving field, are coupled through the damping term $(1/4)\Gamma$. In the absence of damping ($\Gamma=0$), we can directly integrate the equations of motion (B2) and find that the components $U(t,t')$ and $W(t,t')$ oscillate at $+\Omega(t)$ and $-\Omega(t)$, respectively. Proceeding in a manner identical to Blind *et al.* [6], we make the secular approximation, in which we ignore the rapidly oscillating terms, and obtain decoupled equations of motion for $\tilde{U}(t,t')$ and $\tilde{W}(t,t')$, which we can solve by the direct integration. In this approximation, solutions for $U(t,t')$ and $W(t,t')$ can be written in the following form

$$U(t,t')=U(t',t')e^{-[(3/4)\Gamma-i\Omega_0](t-t')-i\Sigma_n A_n(\sin n\delta t'-\sin n\delta t)},$$

$$W(t,t')=W(t',t')e^{-[(3/4)\Gamma+i\Omega_0](t-t')+i\Sigma_n A_n(\sin n\delta t'-\sin n\delta t)}, \tag{B4}$$

where $A_n=2\Omega_n/n\delta$.

We can decompose the modulation terms, which appear in Eq. (B4), into Fourier components [21]

$$e^{\pm iA_n \sin n\delta t'} = \sum_{q_n} J_{q_n}(\pm A_n) e^{iq_n n\delta t'},$$

$$e^{\pm iA_n \sin n\delta t} = \sum_{r_n} J_{r_n}(\pm A_n) e^{ir_n n\delta t}, \tag{B5}$$

where $J_{q_n}(A_n)$ is the $q_n$th order Bessel function.

On using the relation (B5), the solutions (B4) become

$$\begin{aligned} U(t,t') = U(t',t') \sum_{q_1,r_1} \sum_{q_2,r_2} \cdots \sum_{q_p,r_p} & J_{q_1}(A_1) \\ & \times J_{r_1}(-A_1) J_{q_2}(A_2) J_{r_2}(-A_2) \ldots J_{q_p}(A_p) \\ & \times J_{r_p}(-A_p) e^{-[(3/4)\Gamma - i(\Omega_0 + \Sigma_n n q_n \delta)](t-t')} \\ & \times e^{-i\Sigma_n (q_n + r_n) n\delta t}, \end{aligned}$$

$$\begin{aligned} W(t,t') = W(t',t') \sum_{q_1,r_1} \sum_{q_2,r_2} \cdots \sum_{q_p,r_p} & J_{q_1}(A_1) \\ & \times J_{r_1}(-A_1) J_{q_2}(A_2) J_{r_2}(-A_2) \ldots J_{q_p}(A_p) \\ & \times J_{r_p}(-A_p) e^{-[(3/4)\Gamma + i(\Omega_0 + \Sigma_n n q_n \delta)](t-t')} \\ & \times e^{+i\Sigma_n (q_n + r_n) n\delta t}. \end{aligned} \tag{B6}$$

Equation (B6) shows that an $n$th pair of the sideband fields is equivalent to a resonant field with an amplitude of $J_0(A_n)$ plus nonresonant fields at the detuned frequencies $nq_n\delta$ and amplitudes $J_{q_n}(A_n)$.

According to the definition of the fluorescence spectrum (1), we must evaluate the two-time correlation function of the atomic dipole operators. Using Eq. (B1), one finds that the two-time correlation function can be expressed by the linear combinations $V, U$, and $W$ as

$$Y_1(t,t') = V(t,t') - \frac{i}{2}[U(t,t') - W(t,t')]. \tag{B7}$$

Consequently, the double integration in Eq. (1) splits into three parts leading to three distinct components of the spectrum

$$\begin{aligned} S_0(\omega) &= \Gamma \, \mathrm{Re}\left( \frac{1}{T} \int_0^T dt \int_0^t dt' V(t,t') e^{i(\omega - \omega_0)(t-t')} \right), \\ S_{\Omega_0}(\omega) &= -\frac{\Gamma}{2} \mathrm{Re}\left( \frac{1}{T} \int_0^T dt \int_0^t dt' iU(t,t') e^{i(\omega - \omega_0)(t-t')} \right), \\ S_{-\Omega_0}(\omega) &= \frac{\Gamma}{2} \mathrm{Re}\left( \frac{1}{T} \int_0^T dt \int_0^t dt' iW(t,t') e^{i(\omega - \omega_0)(t-t')} \right), \end{aligned} \tag{B8}$$

where $S_0(\omega)$ corresponds to fluorescence at the central frequency $\omega_0$, whereas $S_{\pm\Omega_0}$ correspond to fluorescence at the Rabi sidebands. According to Eqs. (B3) and (B6), the modulation affects only the Rabi sidebands leaving the central component unchanged, independent of the number of the driving fields.

Substituting Eqs. (B3) and (B6) into Eq. (B8) and assuming that $\Omega_0 \gg \Gamma$, we find that in the limit of long-averaging times ($T \to \infty$), the fluorescence spectrum is given by

$$\begin{aligned} S_{in}(\omega) = \frac{1}{8}\Gamma^2 \Bigg[ & 1 - \frac{3}{4}\Gamma^2 \sum_{q_1} \cdots \sum_{q_p} \frac{J_{q_1}^2(A_1), \ldots J_{q_p}^2(A_p)}{\left(\frac{3}{4}\Gamma\right)^2 + \left(\Omega_0 - \sum_n n q_n \delta\right)^2} \Bigg] \Bigg\{ \frac{1}{\frac{1}{4}\Gamma^2 + (\omega - \omega_0)^2} \\ & + \frac{3}{4} \sum_{q_1,r_1} \cdots \sum_{q_p,r_p} \frac{J_{q_1}(A_1) J_{r_1}(-A_1) \ldots J_{q_p}(A_p) J_{r_p}(-A_p)}{\frac{9}{16}\Gamma^2 + \left(\omega - \omega_0 + \Omega_0 + \sum_n n q_n \delta\right)^2} \delta_{q_1 + r_1 + \cdots + pq_p + pr_p, 0} \\ & + \frac{3}{4} \sum_{q_1,r_1} \cdots \sum_{q_p,r_p} \frac{J_{q_1}(A_1) J_{r_1}(-A_1) \ldots J_{q_p}(A_p) J_{r_p}(-A_p)}{\frac{9}{16}\Gamma^2 + \left(\omega - \omega_0 - \Omega_0 - \sum_n n q_n \delta\right)^2} \delta_{q_1 + r_1 + \cdots + pq_p + pr_p, 0} \Bigg\}. \end{aligned} \tag{B9}$$

The spectrum (B9) has been obtained by dropping the contribution to the intensities of the sidebands of the product terms $|Y_2(t',t')|^2$ and $Y_2(t',t')Y_3(t',t')$, which make the spectrum more apparent without introducing any significant errors. It is seen that the spectrum (B9) is composed of three distinct terms: The central component, which is a Lorentzian located at $\omega = \omega_0$, and two multipeak structures centered about $\pm\Omega_0$. The sideband peaks are located at multiplets of $\delta$ and their positions are independent of the number of modulating fields. However, the amplitudes of the sideband lines depend on the number of modulating fields and their Rabi frequencies. Moreover, the dependence of the amplitudes on the Kronecker delta function indicates that only these terms contribute to the spectrum for which

$$q_1 + r_1 + 2q_2 + 2r_2 + \cdots + pq_p + pr_p = 0. \tag{B10}$$

There is an infinite number of the parameters $q_n$ and $r_n$ satisfying the condition (B10). In general, the spectrum (B9) is quite complicated and it is difficult to predict the dependence of the spectral features on the number of modulating fields. However, in the limit of a small number of modulating fields, Eq. (B9) simplifies significantly, and we can explicitly analyze the properties of the fluorescence spectrum.

For $p=1$, the only terms that contribute to the amplitudes of the sideband peaks are those with $q_1=-r_1$. In this case the spectrum reduces to

$$S_{in}(\omega)=\frac{1}{8}\Gamma^2\left[1-\frac{3}{4}\sum_{q_1}\frac{\Gamma^2 J_{q_1}^2(2\Omega/\delta)}{\left(\frac{3}{4}\Gamma\right)^2+(\Omega_0-q_1\delta)^2}\right]\left\{\frac{1}{\frac{1}{4}\Gamma^2+(\omega-\omega_0)^2}+\frac{3}{4}\sum_{q_1}\frac{J_{q_1}^2(A_1)}{\frac{9}{16}\Gamma^2+(\omega-\omega_0+\Omega_0+q_1\delta)^2}\right.$$
$$\left.+\frac{3}{4}\sum_{q_1}\frac{J_{q_1}^2(A_1)}{\frac{9}{16}\Gamma^2+(\omega-\omega_0-\Omega_0-q_1\delta)^2}\right\}. \tag{B11}$$

The spectrum (B11) is essentially the same as those of Blind *et al.* [6]. Since the amplitudes of the sideband lines are proportional to $J_{q_1}^2(A_1)$, the spectrum is invariant under the change of the sign of the modulation amplitude, i.e., $\Omega\rightarrow-\Omega$. For $p>1$, the spectrum becomes sensitive to the sign of the modulation amplitude. We illustrate this for $p=2$, where the spectrum is given by

$$S_{in}(\omega)=\frac{1}{8}\Gamma^2\left[1-\frac{3}{4}\Gamma^2\sum_{q_1}\sum_{q_2}\frac{J_{q_1}^2(2\Omega/\delta)J_{q_2}^2(2\Omega/2\delta)}{\left(\frac{3}{4}\Gamma\right)^2+[\Omega_0-(q_1+2q_2)\delta]^2}\right]$$
$$\times\left\{\frac{1}{\frac{1}{4}\Gamma^2+(\omega-\omega_0)^2}+\frac{3}{4}\sum_{q_1,r_1}\sum_{q_2,r_2}\frac{J_{q_1}(A_1)J_{r_1}(-A_1)J_{q_2}(A_2)J_{r_2}(-A_2)}{\frac{9}{16}\Gamma^2+[\omega-\omega_0+\Omega_0+(q_1+2q_2)\delta]^2}\delta_{q_1+r_1+2q_2+2r_2,0}\right.$$
$$\left.+\frac{3}{4}\sum_{q_1,r_1}\sum_{q_2,r_2}\frac{J_{q_1}(A_1)J_{r_1}(-A_1)J_{q_2}(A_2)J_{r_2}(-A_2)}{\frac{9}{16}\Gamma^2+[\omega-\omega_0-\Omega_0-(q_1+2q_2)\delta]^2}\delta_{q_1+r_1+2q_2+2r_2,0}\right\}. \tag{B12}$$

The spectrum (B12) corresponds to that calculated numerically in Fig. 1(b) and shows that the multipeaked features are not symmetrical about $\Omega_0$ and the structure flips over $\Omega_0$ as $\Omega\rightarrow-\Omega$. The most significant change in the amplitude of the spectral lines is seen in the lines located at $\Omega_0\pm\delta$.


[1] B.R. Mollow, Phys. Rev. **188**, 1969 (1969).

[2] C. Cohen-Tannoudji and S. Reynaud, J. Phys. B **10**, 345 (1977); C. Cohen-Tannoudji, J. Dupont-Roc, and G. Grynberg, *Atom-Photon Interactions* (Wiley, New York, 1992).

[3] For a recent review, see Z. Ficek and H.S. Freedhoff, in *Progress in Optics*, edited by E. Wolf (North-Holland, Amsterdam, 2000), Vol. 40, p. 389.

[4] M.A. Newbold and G.J. Salamo, Phys. Rev. A **22**, 2098 (1980); J. Czub and S. Kryszewski, J. Phys. B **16**, 3171 (1983); K. Rzażewski and M. Florjańczyk, *ibid.* **17**, L509 (1984); E.J. Robinson and P.R. Berman, *ibid.* **17**, L847 (1984); M. Lewenstein, J. Zakrzewski, and K. Rzażewski, J. Opt. Soc. Am. B **3**, 22 (1986); E.J. Robinson, J. Phys. B **19**, L657 (1986); S. Cavalieri, R. Buffa, M. Matera, and M. Mazzoni, *ibid.* **20**, 5363 (1987).

[5] N. Nayak and G.S. Agarwal, Phys. Rev. A **31**, 3175 (1985); M. Wilkens and K. Rzażewski, *ibid.* **40**, 3164 (1989); M. Janowicz, *ibid.* **44**, 3144 (1991).

[6] B. Blind, P.R. Fontana, and P. Thomann, J. Phys. B **13**, 2717 (1980).

[7] M.Z. Smirnov, J. Opt. Soc. Am. B **11**, 109 (1994); T. G. Rudolph, Ph.D. thesis, York University, Toronto, 1998; Z. Ficek and T. Rudolph, Phys. Rev. A **60**, R4245 (1999).

[8] G.Yu. Kryuchkov, Opt. Commun. **54**, 19 (1985); Y. Zhu, A. Lezama, D.J. Gauthier, and T.W. Mossberg, Phys. Rev. A **41**, 6574 (1990); S.P. Tewari and M.K. Kumari, *ibid.* **41**, 5273 (1990); H.S. Freedhoff and Z. Chen, *ibid.* **41**, 6013 (1990); G.S. Agarwal, Y. Zhu, D.J. Gauthier, and T.W. Mossberg, J. Opt. Soc. Am. B **8**, 1163 (1991); Z. Ficek and H.S. Freedhoff, Phys. Rev. A **53**, 4275 (1996); C.C. Yu, J.R. Bochinski,

T.M.V. Kordich, T.W. Mossberg, and Z. Ficek, *ibid.* **56**, R4381 (1997); T. Rudolph, H.S. Freedhoff, and Z. Ficek, *ibid.* **58**, 1296 (1998); M. Jakob, Y. Abranyos, and J.A. Bergou, J. Opt.B: Quantum Semiclass. Opt. **3**, 130 (2001).

[9] A.M. Bonch-Bruevich, T.A. Vartanyan, and N.A. Chigir, Zh. Éksp. Teor. Fiz. **77**, 1899 (1979) [Sov. Phys. JETP **50**, 901 (1979)]; G.I. Toptygina and E.E. Fradkin, *ibid.* **82**, 429 (1982) [ **55**, 246 (1982)]; P. Thomann, Sov. Phys. JETP **19**, 2411 (1976); G.S. Agarwal and N. Nayak, *ibid.* **19**, 3385 (1986); S. Chakmakjian, K. Koch, and C.R. Stroud, Jr., J. Opt. Soc. Am. B **5**, 2015 (1988); W.M. Ruyten, *ibid.* **6**, 1796 (1989); Y. Zhu, Q. Wu, S. Morin, and T.W. Mossberg, Phys. Rev. Lett. **65**, 1200 (1990); Yu. A. Zinin and N.V. Sushilov, Phys. Rev. A **51**, 3916 (1995); S. Papademetriou, S. Chakmakjian, and C.R. Stroud, Jr., J. Opt. Soc. Am. B **9**, 1182 (1992); N.B. Manson, C. Wei, and J.P.D. Martin, Phys. Rev. Lett. **76**, 3943 (1996); B. Lounis, F. Jelezko, and M. Orrit, *ibid.* **78**, 3673 (1997); T.H. Yoon, S.A. Pulkin, J.R. Park, M.S. Chung, and H.-W. Lee, Phys. Rev. A **60**, 605 (1999); T.H. Yoon, M.S. Chung, and H.-W. Lee, *ibid.* **60**, 2547 (1999).

[10] G.S. Agarwal and W. Harshawardhan, Phys. Rev. A **50**, R4465 (1994); W. Harshawardhan and G.S. Agarwal, *ibid.* **55**, 2165 (1997); M.W. Noel, W.M. Griffith, and T.F. Gallagher, *ibid.* **58**, 2265 (1998).

[11] Q. Wu, D.J. Gauthier, and T.W. Mossberg, Phys. Rev. A **49**, R1519 (1994); Q. Wu, D.J. Gauthier, and T.W. Mossberg, *ibid.* **50**, 1474 (1994); P.K. Lam and C.M. Savage, *ibid.* **50**, 3500 (1994); B.M. Garraway and N.V. Vitanov, *ibid.* **55**, 4418 (1997); S.F. Chien, M.R.B. Wahiddin, and Z. Ficek, *ibid.* **57**, 1295 (1998); Z. Ficek, J. Seke, A. Soldatov, and G. Adam, Opt. Commun. **182**, 143 (2000).

[12] G.S. Agarwal, Phys. Rev. A **61**, 013 809 (2000); M. Janowicz, *ibid.* **61**, 025 802 (2000).

[13] H. Friedmann and A.D. Wilson-Gordon, Phys. Rev. A **36**, 1333 (1987); P. Zhou and S. Swain, *ibid.* **55**, 772 (1997); C. Szymanowski, A. Wicht, and K. Danzmann, J. Opt. Soc. Am. B **44**, 1373 (1997); T.H. Yoon and J.R. Park, Phys. Lett. A **264**, 142 (1999).

[14] A.D. Greentree, C. Wei, and N.B. Manson, Phys. Rev. A **59**, 4083 (1999).

[15] J.H. Eberly and K. Wódkiewicz, J. Opt. Soc. Am. **67**, 1252 (1977).

[16] F. Schuda, C.R. Stroud, Jr., and M. Hercher, J. Phys. B **7**, L198 (1974); F.Y. Wu, R.E. Grove, and S. Ezekiel, Phys. Rev. Lett. **35**, 1426 (1975); W. Hartig, W. Rasmussen, R. Schieder, and H. Walther, Z. Phys. A **278**, 205 (1976).

[17] I.S. Gradshteyn and I.M. Ryzhik, *Table of Integrals, Series, and Products* (Academic Press, New York, 1965), p. 38.

[18] Z. Ficek, J. Seke, A. Soldatov, and G. Adam, J. Opt. B: Quantum Semiclass. Opt. **2**, 780 (2000).

[19] M.H. Mittleman, Phys. Rev. A **32**, 276 (1985).

[20] S. Stenholm, *Foundations of Laser Spectroscopy* (Wiley, New York, 1984); S.I. Chu, Adv. At. Mol. Phys. **21**, 197 (1985).

[21] M. Abramowitz and I. Stegun, *Handbook of Mathematical Functions* (Dover, New York, 1972), p. 361.